Prabin Kumar Mahato[1], Swarat Choudhuri[2], Shristi Chaudhary[3], Prashanta Patra[4], Deepak Gupta[5]*

[1]Department of Physics, Ranchi University, Ranchi, India, [2]Department of Physics, St. Xavier College, Ranchi, India, [3]Department of Physics, Chandigarh University, Gharuan, Mohali, Punjab, India, [4]Department of Physics, Kolhan University, Chaibasa, India, [5]School of Basic and Applied Sciences, Galgotias University, Greater Noida, India

Scientific paper
ISSN 0351-9465, E-ISSN 2466-2585
https://doi.org/10.62638/ZasMat1069

Zastita Materijala 66 (3)
584 - 591 (2025)

Morphological, size-dependent field emission investigation of GO and rGO nanosheet

ABSTRACT

Here, we report the role of surface morphologies and grain size on electron field emission characteristics of GO and rGOnanosheets, synthesized through the modified Hummer method. The plasmon peaks were observed at 290nm -310nm for both samples. Here, a plasmonicenergy-associated effective mass model was used to calculate the crystal size of the nanosheet, which is 3.56nm and 4.79nm for GO and rGOnanosheet, which confirms the confinement behavior. Raman data recorded for GO and rGO nanosheet confirm the presence of D and G bands, suggesting growth of GO and rGO, in addition, the Crystal size is calculated by Raman data, which is comparable to Bohr exciton radius size, indicating the GO and rGO are quantum dots. The electron field emission parameters of synthesized GO and rGOnanosheets have been investigated and parameters are calculated by the Fowler–Nordheim (F-N) equation. Among them, the GO sample exhibits the best electron field emission properties with the minimum turn-on voltage of 8.2 V/μm and the field enhancement factor of 1200 due to possessing the smallest emitter tip radius(size) and the varying surface morphologies.

Keywords: *Graphene oxide, Raman, Band gap, Field Emission*

1. INTRODUCTION

Graphene and its derivatives, such as graphene oxide (GO) and reduced graphene oxide (rGO) are said to be effective and promising materials for many applications. Graphene shows a 2D structure, where a uniform, homogeneous single layer of carbon (Z=6) atoms are set in a hexagonal lattice plane and play a significant role in emission properties [1]. Moreover, graphene and its derivatives(GO and rGO) are usually flat with better transmission and efficient charge transfer [2]. Since graphene is getting attraction in nano and tech. fields. Graphene shows high surface area, a variable energy gap, extraordinary thermal as well as electrical conductivity, and excellent mobility at room temperature [3]. The GO is a carbon layer with the presence of oxygen functional, that is attached to both sides of the carbon layer and the carbon edges of the plane [4].GO could be a single or multilayer sheet. A2-dimensional sheet with a single layer is GO; two double layers of GO are named two-layered GO[5]. Moreover, the 2-dimensional GO layer in between two to five layers is called a few-layered GO sheet, and more than five layers are said to be multilayer GO[6]. GO nanosheets are synthesized by the modified Hummer method [7] that controls the morphology and size of nanostructure, which play an important role in electron field emission properties [8].

Electron field emission is the important characteristic of electron emission by the emitter surface height barrier of a structure through the principle of quantum tunnel phenomenon[9]. In the basic theory of thermionic emission(TE), the emitter(GO and rGO) are annealed at extreme temperatures to transfer enough energy to excited electrons, which is needed to discuss the work function of the emitter of the nanosheet [10]. While, the electron field emission is produced under the most intense external applied electricfield to an emitter surface(as cathode), called cold cathode emission [12]. These electron emissions are used for various applications including microwave

*Corresponding author: Prabin Kumar Mahato
Email: pkmahatoru@gmail.com
Paper received: 11.09.2024.
Paper corrected: 22.11. 2024.
Paper accepted: 30.11.2024.

generation devices, gas sensors, field emission displays, and medical imaging [13]. Various groups made an effort to investigate the field emission properties of different nanostructures [9,14,15]. The majority of previously reported investigations on electron field emission of graphene, GO and rGOnanosheetshave not focused in detail. However, the correlation between morphologies and grain size(calculated from the EMA model) with electron field emission propertieshasbeen rarely reported yet.

This investigation reports the role of morphology and grain size on the performance of electron field emission of GO and rGO. The theoretical effective mass models are used to calculate the size using different absorption plasmonic energy. A correlation between morphologies and grain size and electron field emission properties exhibits that the turn-on field is effectively impacted by the size quantum effect in GO and rGOnanosheets.

2. MATERIALS AND METHODS

Graphene oxide (GO) is synthesized through the improved Hummers' method. In the Hummers' method, graphite is oxidized using a mixture of concentrated sulfuric acid (H_2SO_4), sodium nitrate ($NaNO_3$), and potassium permanganate ($KMnO_4$). H_2O_2 is used to stop the reaction. The resultant solution is centrifuged using HCl, and dried in the presence of IR at 85°. Finally, GO is obtained by exfoliating using heat treatment. The oxidation process introduces oxygen-containing functional groups such as hydroxyl (-OH), epoxide (-O-), and carboxyl (-COOH) onto the graphene layers, resulting in the formation of GO.After obtaining GO, reduced graphene oxide (rGO) is prepared by reducing the oxygen-containing functional groups in GO using sodium Borohydride[16-17]. The reduction process removes some of the oxygen groups and partially restores the sp^2 carbon network, leading to the formation of rGO. The schematic of synthesis process is shown in Fig 1.

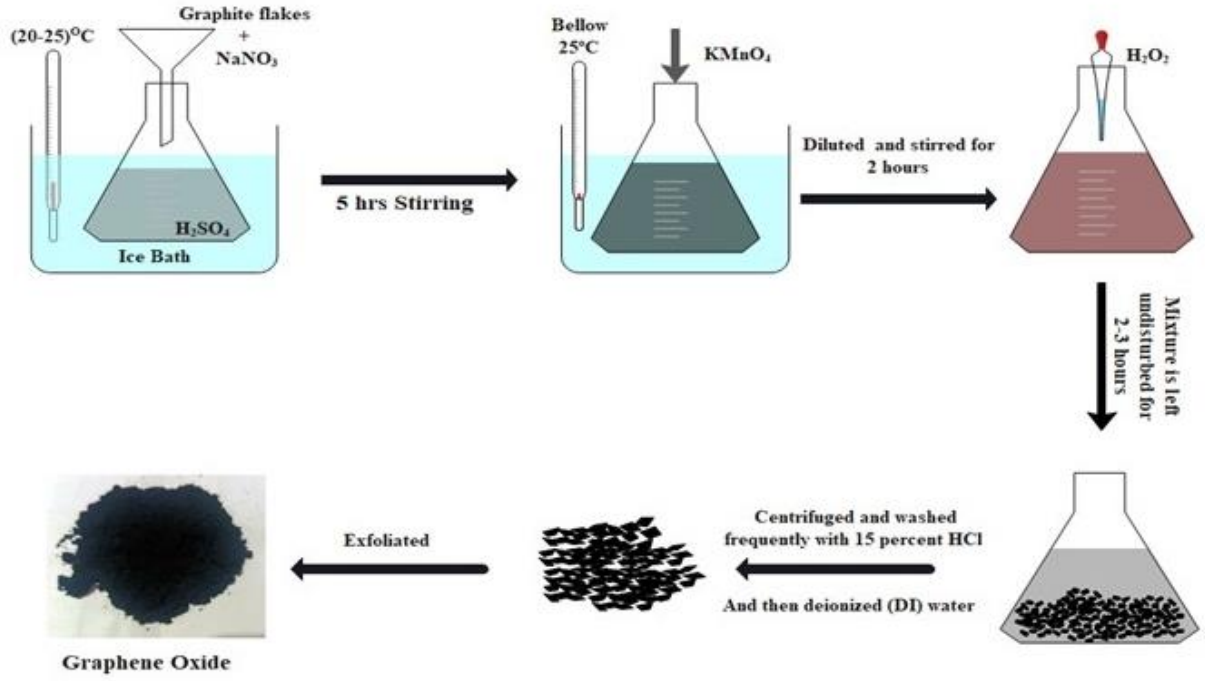

Figure 1. Schematic diagram of synthesis of GO

3. RESULTS AND DISCUSSION

3.1. Morphological and elemental composition of GO and rGO

Figure 2(a-b) displaysthe FESEM micrograph of graphene oxide (GO) and reduced graphene oxide (rGO) samples. Figure 2(a) shows the presence of crumple and spherical type structure, because of the exfoliation of graphite sheet, which becomes to GO nanosheet and results in reduction or deformation onthe exfoliation. Fig. 2(b) displays the micrograph of reduced graphene oxide (rGO), the folded and wrinkled nanostructure has been found. This folding rGOnanosheetis observed on the surface and the edge of rGO due to the losses of the presence of oxygen functional groups[18]. More folded and wrinkled nanosheet is produced when the reduction is quite stronger. A layered sheet with few defects is found in both samples, indicating their polycrystalline behavior. Relatively, the rGOnanosheet shows more aggregation than

the GO. The ratio of C:O for GO and rGO nanosheetshas been investigated through EDS measurement, as shown in Figure 2(c-d). The ratiosof C:O of GO and rGO are 1.48 and 2.53, respectively. The EDS result confirms the reduction of rGO from the GO nanosheet [19].

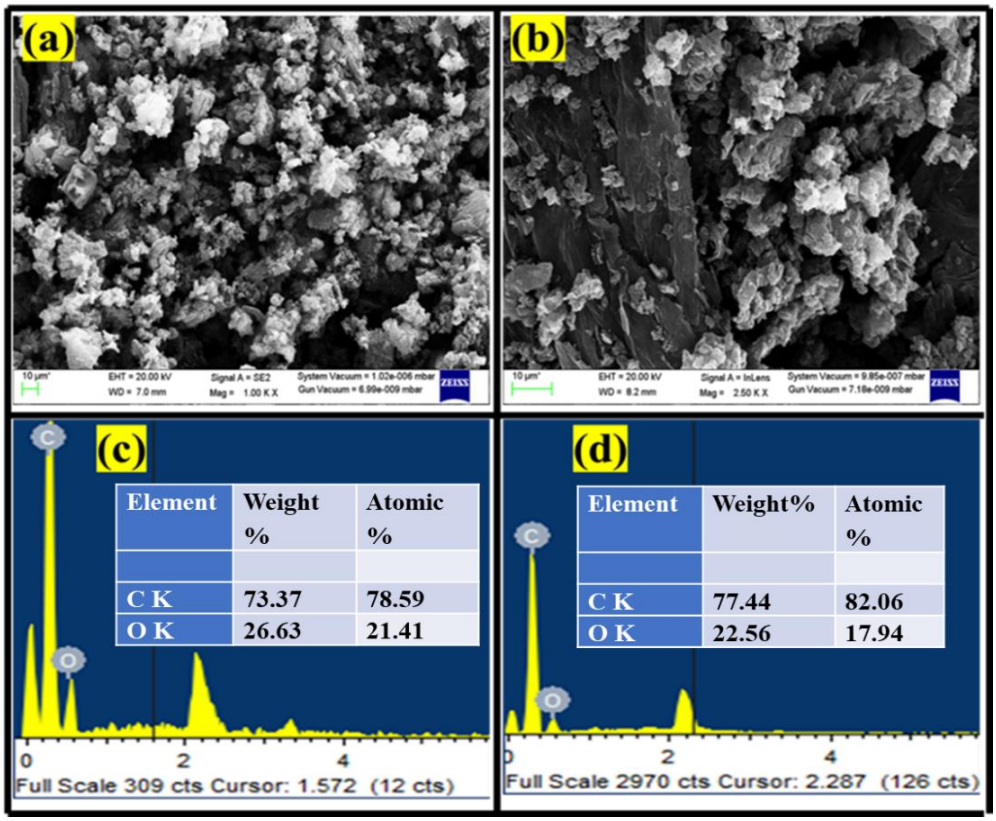

Figure 2. FESEM and EDS spectra,(a-c) GO, (b-d) rGO

3.2. XRD study of GO and rGO

XRD spectra were recorded by using Cu (Kα) radiation (0.154 nm) and intensity was collected in range of 2θ = 5–40◦ for GO and rGOnanosheetto evaluate the structural and elastic properties, as shown in Figure 3. The observed peaks corresponding to reflection planes (001) at 2θ = 11.8 assigned to GO phase and observed peaks corresponding to reflection planes (002) at 2θ = 26.8 assigned to rGOphase [JCPDS card no. 77-2306] .The structural parameters such as crystal size (D), lattice strain (ε), and dislocation density (δ) have been studied corresponding to (001) and (002) reflection peak of GO and rGOnanosheetare estimated using the Scherer equation [20].

$$D = \frac{k\,\lambda}{\beta_D \cos\theta} \qquad (1)$$

$$\varepsilon = \frac{\beta_{hkl}}{4\tan\theta} \qquad (2)$$

Here β_D is full-width at half maximum (FWHM). The estimated average values of D of GO and rGOnanosheetusing Scherrer's formula are 2.9 nm and 6.6 nm. The analysis of disorderness, non-uniformity, non-homogeneity, irregularities and crystal defects present in samples has been carried out using dislocation density (δ), calculated through following equation [21]:

$$\delta = \left(\frac{\beta_D \cos\theta}{k\,\lambda}\right)^2 = \frac{1}{D^2} \qquad (3)$$

The estimated average value of dislocation density of GO and rGOnanosheet are 0.1228 and 0.0229 respectively.

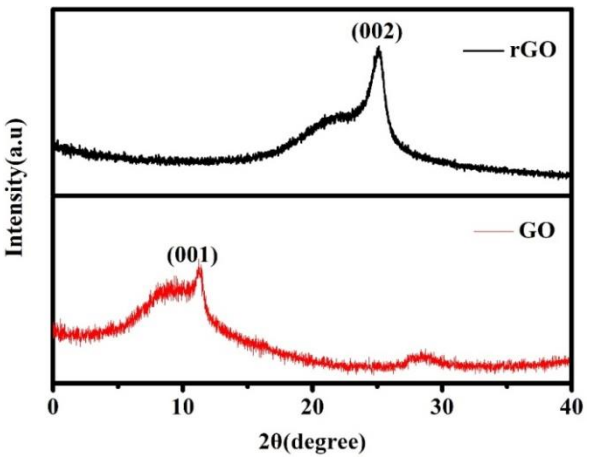

Figure 3. XRDof GO and rGOnanoseet

3.3. Optical and Raman study of GO and rGO

The optical absorption properties of the GO and rGOare shown in Fig. 4(a), The GO exhibits the peak position at 290 nm indicating the p–n* absorption band, on the other hand, the rGO exhibits the peak position at 298 nm indicate the p–n* absorption band, suggest that some groups on the GO nanosheet are eliminated and the conjugated nanostructures have been restored. The surfaceplasmonic position centered at 230 nm for the GO nanosheet is red-shifted(shifting towards a higher wavelength) with increasing reduction i.e GO to rGO samples. Further, red shifting can be explained through the quantum confinement effect through various theoretical models using optical absorption. Here we will use the effective mass model to compute the size, which is expressed as[22-24].

$$E_g^* = E_g^{bulk} - \frac{1.8e^2}{4\pi\epsilon.\varepsilon_r} + \frac{\hbar^2\pi^2}{2r^2}\left(\frac{1}{m_e^*} + \frac{1}{m_h^*}\right) \quad (4)$$

Where r is the crystallite radius.The calculated size from this model are3.56nm and 4.79 nm respectively for both the samples. Besides the effective mass model, another model called the Hyperbolic Band approximation(HBA) model, is used to estimate the size of GO and rGO. The HBA model is expressed as[25-26].

$$E_g^2 = E_{bulk}^2 + \left(\frac{2\hbar^2 E_{bulk}}{\mu}\right)\left(\frac{\pi}{r}\right)^2 \quad (5)$$

The estimated crystallite size from this model is8.45nm and 11.76 nm.

Raman spectroscopy is used to investigate the defects and disorders present in synthesized samples of GO and rGO. Figure 4(b) displays the Raman spectra for both samples, which exhibit two significant bands namely the G band and D band. In the recorded GO and rGO samples, the G band centered at ~1540-1545 cm^{-1}, indcates the perfect GO and rGO nanostructure of a carbon atom with sp^2 hybridization mode and is assigned to E2g-symmetry phonons. The D band is centered at 1350-1380 cm^{-1}, indicating the A1g-symmetry phonons and which confirm the presence of defects in samples. The defect (D) band suggests the disorder in samples arises because of microstructural imperfections and irregularities by the presence of functional groups in the 2-dimensional. graphene sheets. The G-band comes in our samples because of lattice plane vibration of sp^2 hybridized mode of carbon atoms. In the case of the GO nanosheet, the functional groups are fond of the carbon atoms by shifting the hybridization mode from sp2 to sp3mode. On the other hand, the rGO shows the red shifting of the G band than the GO nanosheet. The Raman intensity ratio of D-band (I_D) and G-band (I_G) is also estimated, which gives the information of qualitative assessment of the presence of disorder, defects in the GO and rGO samples. The I_D/I_G ratio decreases from 0.81 to 0.92 for the samples. The I_D/I_Gratio of Raman band decreases with the reduction of graphene oxide. To estimate the grain size from recorded Raman spectra through expression [27]

$$L_a = \frac{560}{E^4}\left(\frac{I_D}{I_G}\right)^{-1}$$

Where E is laser energy and expression $L_a = 2.4*10^{-10}\,\lambda^4\left(\frac{I_D}{I_G}\right)^{-1}$ is used to calculate the size. The estimated Size was 17 and 23 nm for GO and rGO.

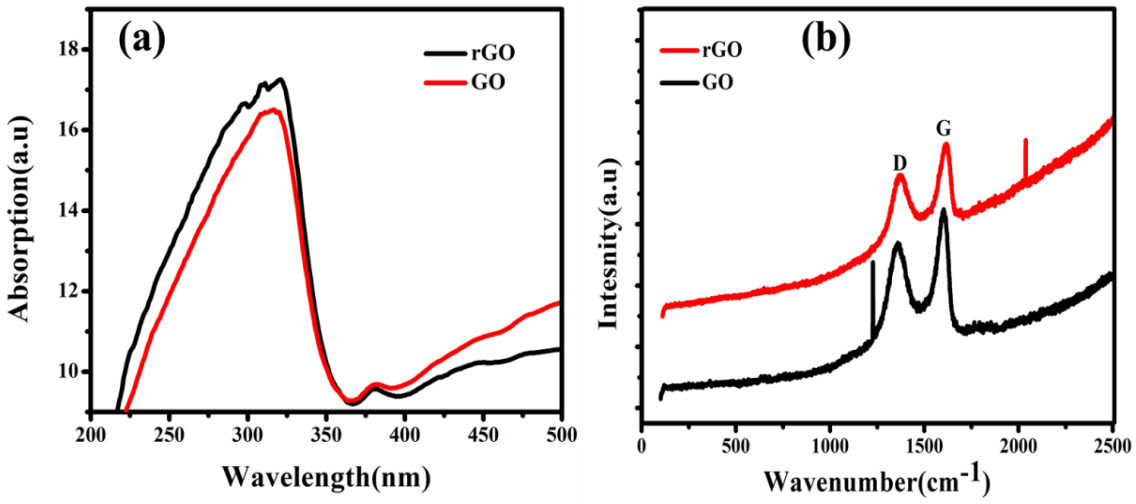

Figure 4. (a) absorption, (b) Raman spectra of GO and rGO

3.4. Field emission properties of GO and rGO

Graphene and its derivatives show promising electron field emission behavior and are examined for application in devices. To understand the emission properties of nanosheets, the electron emissions testing is carried out with diode assembly inside the chamber at a minimum pressure, and the separation between the cathode and anode was0.025cm.A schematic diagram of field emission geometry is shown in Figure 5.

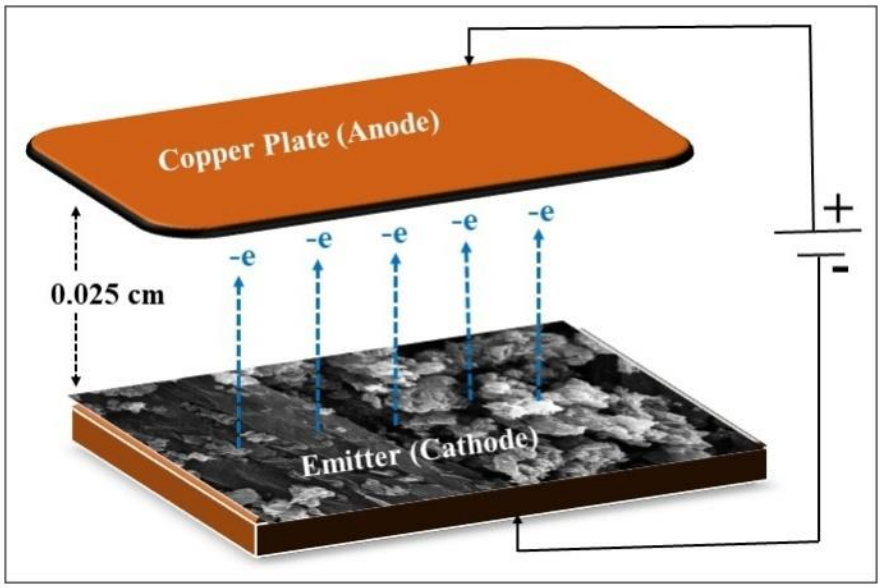

Figure 5. Schematic diagram of field emission geometry

The process of field emission depends on the principle of quantum tunneling phenomenon. Figure 6(a-b) displays the current density (J) versus applied electric field (E) curve plotsfor bothsamples. The turn-on voltage for collection of GO is usually expressed as the electric field needed to create the emission current densities of 15 mA-cm^{-2}. The turn on voltage valuesis found to be 8.67 V/μmand 9.2V/μmfor both the samples. A morphology and size dependent on turn on voltage, indicate that turn-on fields are possibly tailored through tailoring the GO and rGO diameter. A minimum turn on voltage is required for electron field emission from synthesized GO and rGO samples are used for minimal power operation-based devices. It is evidence that the emission behavior of nanosheetis effectively impacted with size. It is required to turn on voltage of GO and rGO shows minimum size because of larger applied external field at the tip of the nanosheet.

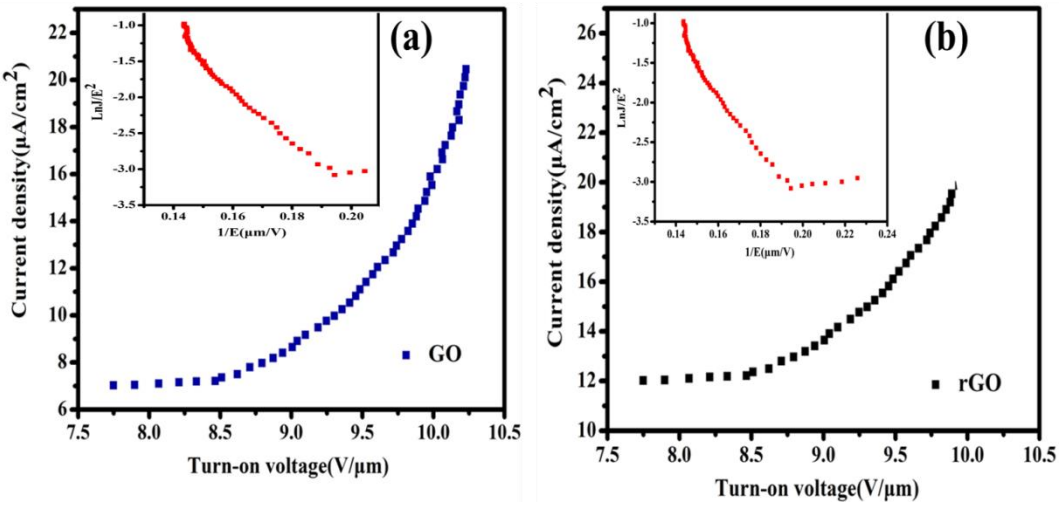

Figure 6. Electron emission current–voltage plot(inset FN plot) of (a) GO, (b) rGO nanosheet

The electron field emission data have been investigated through the Fowler–Nordheim (FN) model which tells about the electron emission current density through barrier tunneling phenomenon, electron field emission current as a function of the applied external electric field and are expressed as follows [28-29].

$$J = \frac{K\beta^2 V^2}{\varphi} exp\left(-\frac{PW^{\frac{3}{2}}}{\beta V}\right) \quad (6)$$

where K (= 1.541 × 10^{-6} $AV^{-2}eV$) is a constant, P = 6831 $eV^{-3/2}\mu m^{-1}$ V, V is the applied electric field, φ is the work function and β is the field-enhancement factor. The plot of ln (J/E^2) with (1/E) is defined as FN plot, whose gradient is expressed as.

$$Gradient = -\frac{P\varphi^{\frac{3}{2}}}{\beta} \quad (7)$$

where, β is field-enhancement factor, which is sued to investigate the degrees of emission enhancement of tips. Various group reported the field-enhancement factor is most significant characteristic, which depends on the surface geometry of the GO and rGO(in our case), and the distance between the emitter(nanosheet) and anode plate. As the effective electron emission area and the φ (work function) for GO and rGO are quite impossible to estimate, field-enhancement factor are calculated by the slope of the fitting FN plot. Inset Figure 5 (a and b)display the FN plot of GO and rGO, which well fitted and the gradient of the linear portion, and further estimated values of field-enhancement factor are 1200 and 1160 for both samples. A size dependent change in turn-on field suggest that electron field emission parameters are also be tailored as a result of size confinement in GO and rGO nanosheet.

4. CONCLUSIONS

This investigation demonstrated the synthetization of GO and rGO through a modified hummer method. XRD pattern confirm the formation of GO and rGO phase. The plasmon peaks were observed at 290 nm to 310 nm for both the samples. Here, a plasmonic energy associated effective mass model was used to calculate the crystal size of nanosheet, which is 3.56nm and 4.79nm for GO and rGOnanosheet, which confirm the confinement behavior. The G band is centered at ~1540-1545 cm^{-1}, and the D band is centered at 1350 to 1380 cm^{-1}, indicating the A1g-symmetry phonons and which confirm the presence of defects in samples. An excellent field emission for GO was found withminimum turn-on voltage of 6 V/μm. The synthesized GOhas proved to be an excellent electron field emitter. On the other hand, the field enhancement factors are 1200 and 1160 for both samples. A maximum field enhancement factor was found for a smaller crystal size sample. A size dependent change in turn-on field suggests that electron field emission parameters are also be tailored as a result of size confinement in GO and rGO nanosheets.

5. REFERENCE

[1] T. M.Magne, T.de Oliveira Vieira, L. M. R.Alencar, F. F. M.Junior, S.Gemini-Piperni, Carneiro, R. Santos-Oliveira(2022)Graphene and itsderivatives: understandingthemainchemical and medicinal chemistry roles forbiomedicalapplications. Journal of nanostructure in chemistry, 12, 693-727. https://doi.org/10.1007/s40097-021-00444-3

[2] R. S.Krishna, J.Mishra, B.Nanda, S. K.Patro, A. Adetayo, T. S.Qureshi(2021) The role of graphene and its derivatives in modifying different phases of geopolymer composites: A review. Construction and Building Materials, 306, 124774. https://doi.org/10.1016/j.conbuildmat.2021.124774

[3] V. B.Mbayachi, E.Ndayiragije, T.Sammani, S.Taj, E. R. Mbuta (2021) Graphene synthesis, characterization and its applications: A review. Results in Chemistry, 3, 100163. https://doi.org/10.1016/j.rechem.2021.100163

[4] J.Liu, S.Chen, Y.Liu, B.Zhao (2022) Progress in preparation, characterization, surface functional modification of graphene oxide: A review. Journal of Saudi Chemical Society, 26(6), 101560. https://doi.org/10.1016/j.jscs.2022.101560

[5] T. R.Mignoli, T. L.Hewer, R. A.Antunes, R. M.Alves, M.Schmal (2021) Synthesis of few-layered graphene sheets as support of cobalt nanoparticles and its influence on CO hydrogenation. Materials Science and Engineering: B, 273, 115388. https://doi.org/10.1016/j.mseb.2021.115388

[6] Y.Cao (2024) Rhombohedral graphene goes correlated at four or five layers. Nature Nanotechnology, 19(2), 139-140. https://doi.org/10.1038/s41565-023-01566-1

[7] N. I.Zaaba, K. L.Foo, U. Hashim, S. J.Tan, W. W. Liu, C. H.Voon (2017) Synthesis of graphene oxide using modified hummers method: solvent influence. Procedia engineering, 184, 469-477. https://doi.org/10.1016/j.proeng.2017.04.118

[8] S.Santandrea, F.Giubileo, V.Grossi, S.Santucci, M. Passacantando, T.Schroeder,... A. Di Bartolomeo (2011) Field emission from single and few-layer graphene flakes. Applied Physics Letters, 98(16). https://doi.org/10.1063/1.3579533

[9] V.Kashyap, C.Kumar, N.Chaudhary, K.Saxena (2022) The role of quantum crystal radius on electron field emission properties of fractal silicon nanowire arrays. Materials Letters, 314, 131842. https://doi.org/10.1016/j.matlet.2022.131842

[10] I.Lahiri, V. P.Verma, W.Choi(2011) An all-graphene based transparent and flexible field emission device. Carbon, 49(5), 1614-1619. https://doi.org/10.1016/j.carbon.2010.12.044

[11] C.Kumar, V.Kashyap, A.Kumar,A. K.Sharma, D.Gupta, D. P.Singh, K.Saxena (2023) Reframe of Fowler-Northeim Approach for Electron Field Emission of a Vertical Silicon Nanowires. Silicon, 15(15), 6591-6602. https://doi.org/10.1007/s12633-023-02505-4

[12] V.Kashyap, C.Kumar, N.Chaudhary, K. Saxena (2023) Quantification of deviation of size dependent field enhancement factor of silicon nanowires array through theoretical modeling. Silicon, 15(3), 1203-1210. https://doi.org/10.1007/s12633-022-02068-w

[13] S.Nirantar, T.Ahmed, M.Bhaskaran, J. W.Han, S. Walia, S. Sriram(2019)Electron emission devices for energy-efficient systems. Advanced Intelligent Systems, 1(4), 1900039. https://doi.org/10.1002/aisy.201900039

[14] Y. W. Zhu, H. Z.Zhang, X. C.Sun, S. Q.Feng,J.Xu, Q. Zhao, ... D. P.Yu (2003) Efficient field emission from ZnOnanoneedle arrays. Applied Physics Letters, 83(1), 144-146. https://doi.org/10.1063/1.1589166

[15] L.Chen, H.Yu, J.Zhong, J.Wu, W.Su (2018) Graphene based hybrid/composite for electron field emission: a review. Journal of Alloys and Compounds, 749, 60-84. https://doi.org/10.1016/j.jallcom.2018.03.100

[16] S. N.Alam, N.Sharma, L. Kumar(2017) Synthesis of graphene oxide (GO) by modified hummers method and its thermal reduction to obtain reduced graphene oxide (rGO). Graphene, 6(1), 1-18. http://dx.doi.org/10.4236/graphene.2017.61001

[17] T. K.Kuanyshbekov, K.Akatan, S. K. Kabdrakhmanova, R.Nemkaeva, M.Aitzhanov, A.Imasheva, E. Kairatuly (2021)Synthesis of graphene oxide from graphite by the hummers method. Oxidation Communications, 44 (2).

[18] N.Sharma, V.Sharma, Y.Jain, M.Kumari, R.Gupta, S. K. Sharma, K.Sachdev (2017) Synthesis and characterization of graphene oxide (GO) and reduced graphene oxide (rGO) for gas sensing application. In Macromolecular symposia. 376(1), 1700006. https://doi.org/10.1002/masy.201700006

[19] N.Aslan, B.Aksakal (2021) Effect of graphene reinforcement on hybrid bioceramic coating deposited on the produced porous Ti64 alloys. Journal of Porous Materials, 28(4), 1301-1313. https://doi.org/10.1007/s10934-021-01081-5

[20] C. Kumar, M.Shrivastav, J.Escrig, L. P.Campos,A. I. Martinez, H.Silva, A. Zarate (2024) The investigation of thickness-dependent mono-fractal, optical and optoelectronics properties of sputtered silver thin film for silicon solar cell. Vacuum, 225, 113247. https://doi.org/10.1016/j.vacuum.2024.113247

[21] V.Kashyap, H.Pawar,I.Sihmar, C.Kumar, A.Kumar, S.Kumar, ... K.Saxena (2024) X-ray analysis of Ag nanoparticles on Si wafer and influence of Ag nanoparticles on Si nanowire-based gas sensor. Applied Physics A, 130(4), 238. https://doi.org/10.1007/s00339-024-07379-w

[22] V.Kashyap,C.Kumar, N.Chaudhary, N.Goyal, K. Saxena (2021) The correlation of resistivity with the crystal size present in silicon nanowires through confinement-based models. Materials Letters, 301, 130312. https://doi.org/10.1016/j.matlet.2021.130312

[23] P.Patra, R.Kumar, C.Kumar, P. K.Mahato (2022)Ni-incorporated cadmium sulphide quantum dots for solar cell: an evolution to microstructural and linear-nonlinear optical properties. Journal of Crystal Growth, 583, 126542. https://doi.org/10.1016/j.jcrysgro.2022.126542

[24] S.Pathak, S.Chaudhary, M.Shrivastav, N.Kumar, S. Varshney, M.Kumar, ... C. Kumar(2024) The effects of air-annealing on the performance of optical-electrical assessment of sputtered CdS film towards the Ag/n-CdS/p-Si (100)/Al photodetectors. Optical Materials, 150, 115117. https://doi.org/10.1016/j.optmat.2024.115117

[25] C.Kumar, V.Kashyap, M.Shrivastav, F.Guzman, D. P.Singh, K.Saxena (2023) In-depth opto-electrical analysis of Ni: CdS film towards the performance as Ag/Ni:CdS/FTOSchottky diode. Optical Materials, 143, 114226. https://doi.org/10.1016/j.optmat.2023.114226

[26] P.Patra, R.Kumar, C.Kumar, K.Pandey, P. K.Mahato (2023)Exploration of impact of thermal condition on microstructural-optical-electrical properties of Ni doped CdS thin films. Materials Today: Proceedings.

[27] https://doi.org/10.1016/j.matpr.2023.07.018

[28] P. K.Mahato, S.Choudhuri, C.Kumar, S.Roy, P. Patra (2023) Evaluation of crystal size present in graphene oxide quantum dots using optical and Raman spectroscopy. Materials Today: Proceedings, 80, 668-673.

[29] V.Kashyap, C.Kumar, V.Kumar, N.Chaudhary, K.Saxena(2022) Induced quantum-Fano effect by Raman scattering and its correlation with field emission properties of silicon nanowires. Applied Physics A, 128(4), 312. https://doi.org/10.1007/s00339-022-05415-1

[30] C.Kumar, V.Kashyap, J. M.Shrivastav, V.Kumar, F.Guzman, K.Saxena(2024) The dopant (n-and p-type)-, band gap-, size-and stress-dependent field electron emission of silicon nanowires. Physical Chemistry Chemical Physics, 26(25), 17609-17621. doi:10.1039/D4CP00825A

IZVOD

MORFOLOŠKO ISTRAŽIVANJE EMISIJE GO I rGO NANOLISTA ZAVISNO OD VELIČINE

Ovde izveštavamo o ulozi morfologije površine i veličine zrna na karakteristike emisije elektronskog polja GO i rGO nanolistova, sintetizovanih modifikovanom Hamerovom metodom. Plazmonski vrhovi su primećeni na 290 nm -310 nm za oba uzorka. Ovde je korišćen model efektivne mase povezan sa plazmonično energijom za izračunavanje veličine kristala nanolima, koja je 3,56 nm i 4,79 nm za GO i rGOnanolist, što potvrđuje ponašanje zatvaranja. Ramanovi podaci snimljeni za GO i rGOnanosheet potvrđuju prisustvo D i G traka, što sugeriše rast GO i rGO, pored toga, veličina kristala se izračunava Ramanovim podacima, koji je uporediv sa veličinom radijusa Borovog eksitona, što ukazuje da su GO i rGO kvantne tačke. Istraženi su parametri emisije elektronskog polja sintetizovanih GO i rGOnano listova i parametri su izračunati pomoću Fauler–Nordhajmove (F-N) jednačine. Među njima, GO uzorak pokazuje najbolja svojstva emisije elektronskog polja sa minimalnim naponom uključivanja od 8,2 V/mm i faktorom poboljšanja polja od 1200 zbog posedovanja najmanjeg radijusa (veličine) vrha emitera i različite morfologije površine.

Ključne reči: *Grafen oksid, raman, pojasni razmak, emisija polja*

Naučni rad
Rad primljen:11.09.2024.
Rad korigovan: 22.11.2024.
Rad prihvaćen: 30.11.2024.

Prabin Kumar Mahato: http://orchid.org/0000-0001-6718-4893
PrashantaPatra: http://orchid.org/0000-0002-2425-1037
DeepakGupta: http://orchid.org/0000-0002-4228-2523